

High Mass Resonance Searches at CDF

Kenichi Hatakeyama

Rockefeller University, New York, NY 10065, USA.

for the CDF Collaboration

Recent searches for dijet, dielectron, and dimuon resonances by the CDF Collaboration are presented. No evidence for a signal is found in any channel, so 95% confidence level upper limits are set on the new particle production.

1. Introduction

Many models beyond the standard model (SM) predict the presence of new heavy particles which can potentially be observed as narrow resonances in the invariant mass spectra of high p_T objects. The Randall-Sundrum (RS) graviton (G^*) in the RS model, Z' , W' , excited quarks (q^*) in the quark compositeness model, axigluon (A) in the chiral color model, coloron (C) in the flavor universal coloron model, color-octet mass-degenerate techni- ρ (ρ_{TS}) in the technicolor model, and the diquark (D) in the E_6 model are such examples. Below, recent searches for narrow resonances in the dijet and dilepton channels are presented.

2. Dijet Mass Resonance Search

CDF recently performed a search for dijet mass resonances using 1.1 fb^{-1} of jet trigger data [1]. Jets are clustered using the cone-based midpoint jet clustering algorithm with cone radius $R_{cone} = 0.7$, and we form dijet mass (m_{jj}) spectrum in events with $|y^{jet1,2}| < 1.0$. After correcting jet energies for the calorimeter non-linearity and non-uniformity effects, a m_{jj} spectrum is formed from the leading two jets, which is further corrected for the bin-by-bin migration effect due to the finite resolution in the m_{jj} measurement. The background (BG) in this search is dominated by QCD dijet production. The measured spectrum is compared to the next-to-leading order QCD predictions in Fig. 1. They are in good agreement.

Narrow mass resonances are searched for in the measured dijet mass spectrum by fitting the spectrum to a smooth functional form $d\sigma/dm_{jj} = p_0(1-x)^{p_1}/x^{p_2+p_3 \ln(x)}$, $x = m_{jj}/\sqrt{s}$, which provides a good description of dijet mass spectra from QCD predictions, and by looking for data points that show significant excess from the fit. The fit of this form to the measured spectrum shows no significant excess.

Limits on the new particle production cross sections are set on $\sigma \cdot \mathcal{B}(X \rightarrow jj) \cdot \mathcal{A}(|y^{jet1,2}| < 1)$. The m_{jj} distributions from q^* , G^* , W' , Z' have different decay modes and thus different signal shapes; therefore, limits are computed using these four signal shapes separately and shown in Fig. 2 together with predictions from various models. This search sets the most stringent mass exclusions on the production of q^* , A , C , D , and ρ_{TS} , which are $260 < m_{q^*} < 870 \text{ GeV}/c^2$ [2], $260 < m_{A/C} < 1250 \text{ GeV}/c^2$, $290 < m_D < 630 \text{ GeV}/c^2$, and $260 < m_{\rho_{TS}} < 1100 \text{ GeV}/c^2$ [3], respectively.

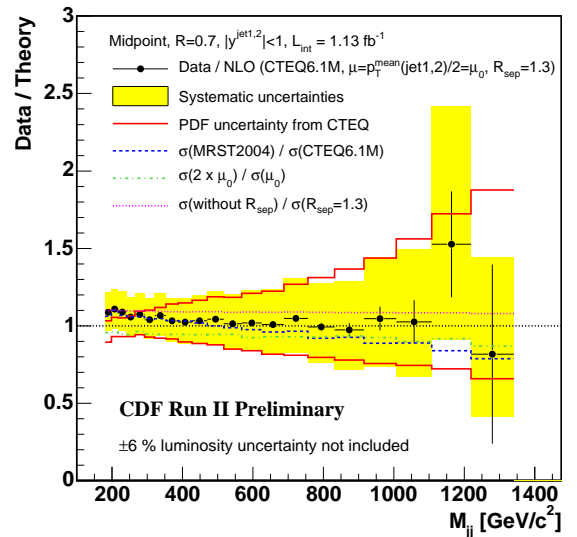


Figure 1: The ratio of the data to the NLO pQCD predictions versus dijet mass.

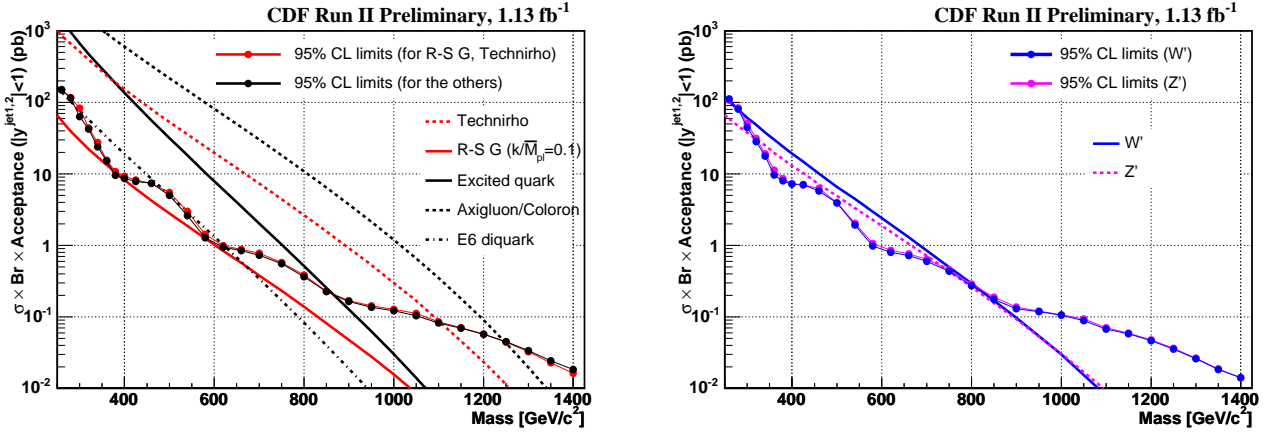


Figure 2: 95% C.L. upper limits on $\sigma \cdot \mathcal{B}(X \rightarrow jj) \cdot \mathcal{A}(|y^{jet1,2}| < 1)$ obtained with the signal shapes from the W' , Z' , G^* , and q^* production compared to various theoretical predictions.

3. Dielectron Resonance Search

CDF reported a new search [4] for dielectron resonances using 2.5 fb^{-1} of data collected by triggering on one or two electromagnetic (EM) clusters. Offline, events are required to have two isolated electrons with $E_T > 25 \text{ GeV}$, one in the central ($|\eta| < 1.1$) region and the other one in either the central or the plug ($1.1 < |\eta| < 2.0$) regions.

The dominant BG in this search is Drell-Yan production of e^+e^- pairs, which is irreducible. Another is dijets and W +jets production (QCD BG) where one or more jets are misidentified as electrons. Other contributions include $Z/\gamma^* \rightarrow \tau\tau$, $t\bar{t}$, and diboson ($W\gamma, WW, WZ, ZZ, \gamma\gamma$) production (other SM BGs). The Drell-Yan and other SM backgrounds are estimated based on Monte Carlo (MC), while the QCD BG is estimated by a data-driven method.

Fig. 3 shows the observed e^+e^- invariant mass spectrum from 2.5 fb^{-1} data together with the expected backgrounds. The most significant deviation between the data and the SM prediction occurs at $m_{ee} = 241.3 \text{ GeV}/c^2$. The probability of finding an excess larger than the observed one from BG only is found to be 0.6% corresponding to 2.5σ . The 95% C.L. limits on $\sigma \cdot \mathcal{B}(X \rightarrow e^+e^-)$ for spin-1 (e.g., Z' 's) and spin-2 (e.g., G^*) particles obtained from this search are presented in Ref. [4].

4. Dimuon Resonance Search

CDF performed a new search for dimuon resonances using 2.3 fb^{-1} of data. The data are collected online by requiring a track matched with muon detector hits, and offline, events with two muons with $p_T > 30 \text{ GeV}/c$ are selected.

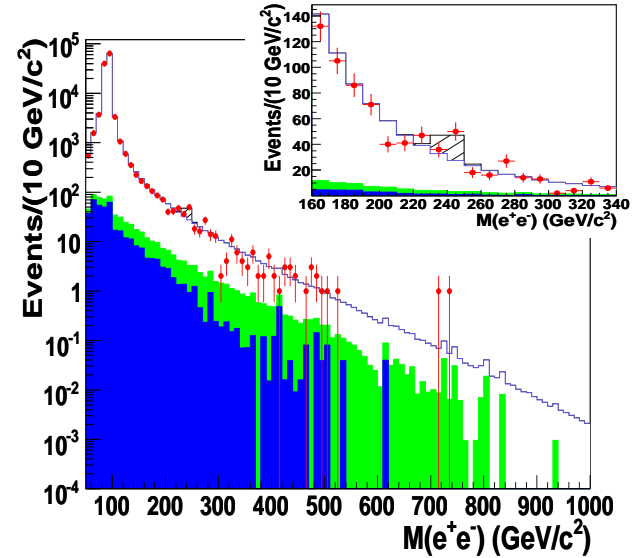


Figure 3: Observed e^+e^- invariant mass distribution compared to the estimated expected backgrounds in a log scale. (inset) The same for the $240 \text{ GeV}/c^2$ region using a linear scale. The hatched histogram shows the expected signal from a $240 \text{ GeV}/c^2$ spin-1 particle normalized to twice the number of excess events seen in the data.

The main BG in this search comes from Drell-Yan production of dimuons. The W^+W^- and $t\bar{t}$ processes also have small contributions. These contributions are estimated based on Pythia MC. The hadron fake contributions (π/K decays-in-flight) are evaluated based on same sign dimuon pairs, and the backgrounds come from cosmic-rays are estimated using track timing information.

In this search, $1/m_{\mu\mu}$ distribution is formed instead of $m_{\mu\mu}$ distribution as shown in Fig. 4, since at high mass, the $m_{\mu\mu}$ resolution is dominated by the track curvature resolution, resulting in an approximately constant resolution in $\delta(1/m_{\mu\mu})$. The signal is searched for by constructing the $1/m_{\mu\mu}$ distribution templates for Z' boson pole masses, adding the background distributions to the templates, and comparing them to the $1/m_{\mu\mu}$ distribution from data in the search region $1/m_{\mu\mu} < 10$ (TeV/c²)⁻¹.

Fig. 4 shows good agreement between data and expected backgrounds. The 95% C.L. limits on $\sigma \cdot \mathcal{B}(X \rightarrow \mu^+\mu^-)$ for spin-1 and spin-2 particles are shown in Fig. 5 together with theoretical predictions for various Z' 's and G^* 's with several k/M_{pl} values. This search provides the most stringent constraints on Z' 's in various models and on G^* .

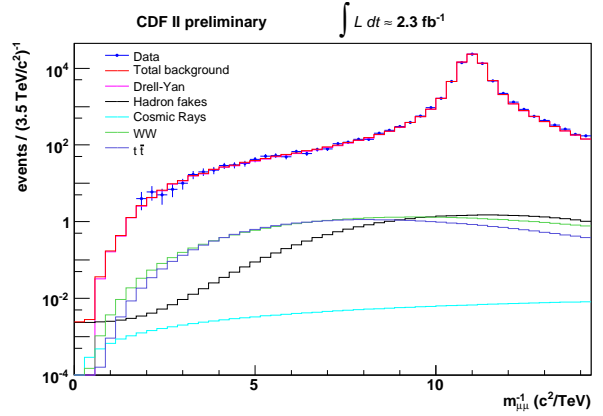


Figure 4: Observed $1/m_{\mu\mu}$ distribution from 2.3 fb⁻¹ of data compared to the estimated backgrounds.

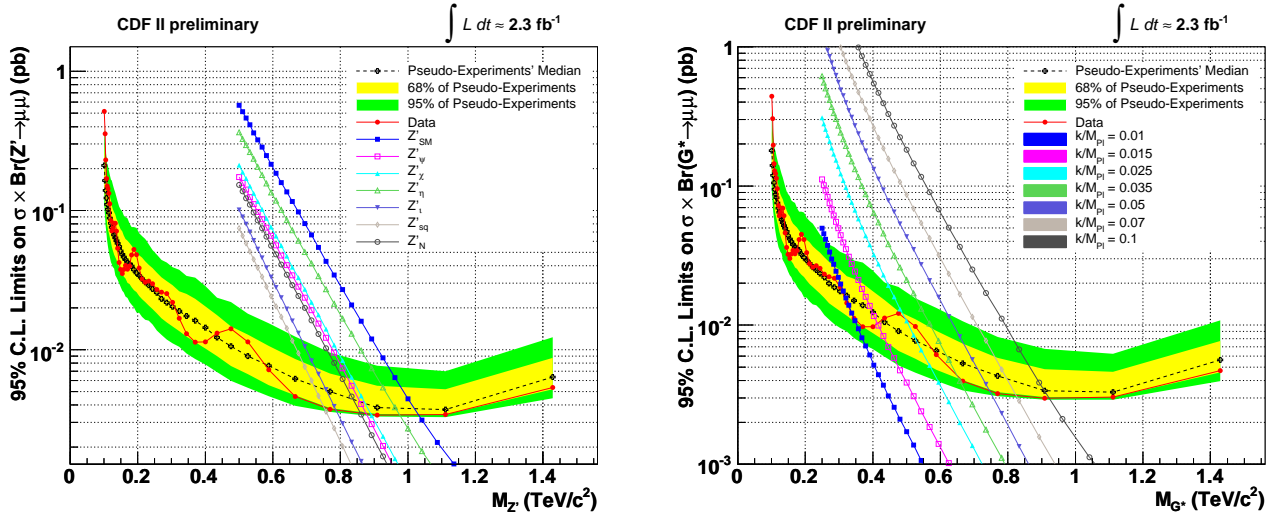


Figure 5: The upper limits on $\sigma \cdot \mathcal{B}$ at 95% C.L. for spin-1 particles from the m^+m^- data (left), and on spin-2 particles from the m^+m^- data (right).

References

- [1] CDF Collaboration, CDF public note 9246.
- [2] The following couplings are used: $f = f' = f_s = 1$.
- [3] The following parameters are used: $M'_8 = 0$, $M(\pi_{22}^8) = 5M(\rho_{T8})/6$, $M(\pi_{22}^1) = M(\pi_{22}^8)/2$ and $M_8 = 5M(\rho_{T8})/6$.
- [4] T. Aaltonen *et al*, CDF Collaboration, arXiv:0810.2059, submitted for publication in Phys. Rev. Lett.
- [5] O. Stelzer-Chilton, CDF Collaboration, this proceeding.